

INDUCTION WELDING TAKES NEW AIM FOR REINFORCED THERMOPLASTICS IN HIGH STRENGTH AND LOAD BEARING APPLICATIONS

Russell J. Nichols, Ashland Specialty Chemical Co., Norwood, New Jersey 07648, USA
Val A. Kagan, Technical Adviser, New Jersey 07950-1960, USA

Abstract

Recent developments in magnetic implant induction welding have focused on optimizing mechanical performance of joints in reinforced plastics through continuous improvement to the welding technology (including magnetic implant material properties, SPC process control, joint design optimization, etc.). In this study, 33 wt. % fiber-glass reinforced Nylon 6 was used in a chain-optimization study to conduct a critical comparison of two alternatives for thermoplastic welding. Results demonstrate interactions between material composition, joint design, and welding process conditions.

Introduction

All methods of welding thermoplastics described in the technical literature [1-2] share one fundamental characteristic: a layer of molten material must be created at the interface between the parts for weld inter-phase formation to occur. The various technologies that exist for welding thermoplastics differ primarily by the means used to introduce energy to the bond line. These means can be divided into the following three groups:

- Mechanical movement (frictional: linear and orbital, spin, ultrasonic, kinetic, etc.).
- External (hot plate, hot bar, hot gas/air, extrusion, over-molding).
- Electromagnetic (induction, high frequency, and infrared/laser, etc.).

Aspects of part design, end-use performance, and material composition (including the performance impact of reinforcements and other additives) all play a role in determining which heat generation method is preferable for any specific application. In this study the mechanical strength performance of 33 wt. % fiber-glass reinforced Nylon 6 parts with linear vibration butt-welded joints is compared to that of comparable parts with magnetic implant induction welded (Emabond™)¹ tongue-in-groove shear joints. The geometry of the parts used in the study was the same injection molded two-shelf system (“Cereal Bowls”) as that used in a previous comprehensive study [3] on efficiency of linear vibration welding of fiber-

glass reinforced nylon. Because the parts were injection molded using a common mold assembly (the only changes were different insert rings to define the joint details), the imposed stresses on the two types of joints were as similar as possible.

Typically, frictional welding methods require use of butt-joint configurations. Although many joint types (including butt-welds) are used for induction welding, one of the strongest, and hence most frequently used joints is the tongue-in-groove design. Both the butt-joint and the tongue-in-groove joint designs (Figure 1) have limitations in their execution that limit the ultimate strength of the joint. In the case of linear vibration welded butt-joints, the limiting factor is joint width (imposed by the wall thickness). In the case of the induction welded tongue-in-groove joint, the joint performance is related to the length and thickness of the tongue [4].

In a previous study of vibration welding for nylon-based plastics, it was reported [2] that for glass-fiber reinforced nylon, the maximum weld strength of a butt-joint is approximately equal to the strength of the base polymer/matrix (Figure 2). It was also shown that there is a further decrease in mechanical properties due to the trade-off imposed by the use of impact modifiers, where strength is sacrificed to gain ductility.

Induction Welding Principles

Induction welding of thermoplastic materials has been in commercial use for over twenty years [4-5]. Systems range in complexity from highly automated multi-station units with integrated robotic material handling to simple single-station units with manual loading and unloading of parts. In all cases, the heating is generated by an RF induction field in the 2-10 MHz frequency range acting upon a magnetic susceptor implant.

In principle, any thermoplastic polymer that melts on heating can be welded by the induction welding process. In practice, the technology has been applied most widely to the polyolefins and recently has found growing use in engineering thermoplastics such as Nylon 6 in load bearing or high strength applications.

¹ Emabond™ - is trade name of Ashland Specialty Chemical Company

The means by which energy is *induced* (i.e., transferred) to the bondline is similar in concept to the function of an electrical transformer. In a transformer, two separate coils (or windings) are placed around a magnetically susceptible core (typically ferrite). It is possible to induce (AC) current between closely adjacent coils even when the apparent core material is air. When AC current is applied to one of the windings, the other winding is energized even though no obvious current path exists between the two coils. It is magnetic induction that causes those phenomena to occur. In this system, radio frequency (RF) energy is applied through a coil that conforms closely to the bondline of the parts to be joined. Energy absorbed by the magnetic susceptor material placed in the bondline provides intense, controllable, local heating directly at the joint interface. It is also possible to optimize the transfer of energy from the RF coil to the susceptor material by directing the magnetic lines of flux through use of reflector coils (non-energized coils that “reflect” the magnetic lines of force to the bondline).

Heating occurs principally by hysteresis loss [5], and to a slight degree, by eddy current (or I^2R) heating of the particulate ferromagnetic susceptor applied at the bondline. The heating rate is determined by the magnetic permeability, or magnetic susceptibility, of the implant at the bond interface. The magnitude of the hysteresis loss is described by the area enclosed in a plot of the induction field (B) versus the magnetic field (H) as shown in Figure 3. The reason that high frequency is required for efficient heating is that even with a susceptor with optimal magnetic properties, the amount of heating that occurs in a single hysteresis loop is miniscule (on the order of 0.003 °C).

The interrelationship between the geometry of the joint and the spatial positioning of the RF coil determines the overall efficiency of energy transfer from the RF coil to the magnetic susceptor material placed in the joint. The reflector is a non-energized coil that directs the magnetic lines of flux toward the bondline. The parts to be joined are also subject to a modest clamping force during joining to assure adequate flow of the susceptor material, and containment of the parts during cooling.

Experimental Procedure

The geometry of the parts used in the study was the same injection molded two-shelf system (“Cereal Bowls”) as that used in a previous study of linear vibration welding of fiber-glass reinforced nylon [3]. For the present study on induction welding technology using a tongue-in-groove joint, a tongue, 3.4 mm thick and 6.65 mm long, is molded into the upper shell and a mating groove is molded into the lower shell. Figure 4 shows a sequence of photographs of the fixture and RF coil used for the study. The first view

shows the RF coil, the second view shows the lower half of the “Cereal Bowl” placed in the coil, the third view shows the upper half of the “Cereal Bowl” in place atop the lower half (with the tongue engaged in the groove), and the final view shows the placement of the non-energized reflector (or attenuator) coil.

Prior to initial welding trials, thermal imaging was used to characterize the heating performance of the susceptor compound in the open groove of a part with the RF field applied. Individual images can be used to identify heating uniformity throughout the part, or multiple images of a specific location can be tracked and plotted to identify heating rate as a function of time. Figure 5 is a typical (instantaneous) thermal scan obtained using a FLIR Systems Thermacam SC300 long wave focal plane array (FPA) thermal analysis package.

Initial process conditions were established by performing a screening DOE. In this case, a two-factor, two-level, fractional factorial experimental design with an added center point and three replicates was selected. The two factors used in the initial DOE were weld time and low pressure set-point. A contour plot of the screening DOE result is shown in Figure 6. In this case, the screening DOE indicated that reductions in both weld time and low pressure set-point were required to further optimize burst pressure.

After the initial screening was completed, further process refinements were added to optimize welding performance: weld time @ low pressure 0.14 MPa (20 PSI) cylinder pressure, weld time @ high pressure 0.62 MPa (90 PSI) cylinder pressure, and cooling time.

Mechanical Performance Data

The welded test samples were connected to a Barbee P-200 portable hydrostatic tester, at room temperature. The welded sample was initially filled with room temperature water and then pressurized with air. The air pressure was applied by a manually operated ball valve. The burst pressure was recorded using a 0-2.76 MPa (0-400 PSI) Noshok[®] oil-filled pressure gauge with a re-settable indicator. Burst testing was conducted within one hour of induction welding.

Following a chain optimization, a series of bowls were welded at the optimized test conditions. The optimized conditions were identified as 11 seconds weld time at low pressure, 5 seconds weld time at high pressure, and 20 seconds cooling time. The low pressure force applied during welding was 186.5 kgf per meter (10.5 LBf per inch) of bondline. The high pressure force applied was 840.5 kgf/m (47.1 LBf/in) of bondline.

Average burst strength of 1.33 MPa (192 PSI) was observed with a maximum burst strength of 1.50 MPa (218 PSI) and a minimum burst strength of 1.22 MPa (177 PSI). Figure 7 further summarizes the comparative welding performance of induction welding and vibration welding. The comparative vibration welding data was reported in previous study of linear vibration welding of fiber-glass reinforced nylon [3].

Failure Mode Analysis

Mechanical performance of the induction welded cereal-bowl system by the burst pressure criteria depends both on the level of reinforcement and on local distribution of the reinforcing materials in the tongue and groove sections. As a result of both joint design and process optimization activities, the common failure mode found among these samples was fracture through the tongue (Figure 8). The specimens with fractures through the lower end (nearer the tip) of the tongue correspond with lower burst strengths, while fractures through the upper end (nearer the root) of the tongue correspond with the higher burst strengths. Fracture through the tongue implies a flexural affect related to the geometry of the bowl system, rather than just a local joint geometry issue. Further, it is evident that the strength of the tongue is dependent upon the fiber-glass orientation and distribution.

Conclusion

The recent developments focused on the optimization of mechanical performance of induction welded fiber-glass reinforced nylon 6.

- These data demonstrate that induction welding can meet increased performance demands while also minimizing the wall thickness. Induction welding provided an overall improvement in average burst strength of 25% versus historical data.
- The common failure mode observed, fracture through the tongue, suggests that further strength optimization can be obtained by redesign of the joint to increase the thickness of the tongue, even within the overall joint width constraints of the present bowl design.
- The apparent strength limitation in this element appears to be dependent upon the distribution of the reinforcing glass fibers in the local region.
- A larger cross-section in the tongue would also assure better distribution of glass fibers during the injection molding process.
- It is believed that this data is generally applicable to other fiber-glass reinforced plastic systems.

It is hoped that the results presented in this study will help plastic part designers, material developers, and manufacturers choose optimized induction welding conditions for reinforced engineering thermoplastics parts in a wide range of high-strength and load bearing applications.

Acknowledgments

The authors wish to thank Juan Ruiz for injection molding, Rommel Velasco, Brian Agosto, and Joshua Guerra for welding and testing, and Raymond Trunk for tooling. Special thanks go to Drew P. LaMarca and Steve Chookazian for help in preparing this study for publishing. Their contributions are greatly appreciated.

References

1. *Plastics and Composites Welding Handbook*, Edited by D. A. Greweel, A. Benatar, and J. Park, 407 pages, Hanser Publisher, Munich (2003).
2. Kagan, V., "Alternatives for Joining Technologies for Under-the-Hood Plastic Parts: From Linear Vibration to Laser Transmission Welding", *POWERTRAIN INTERNATIONAL*, **3:3** 24-35, (2000).
3. Lee, C. and Kagan, V., "Angular Variation of Vibration Weld Joint Strength: In Horizontal Plane and in Vertical Plane", SAE Technical Paper Series # 2002-01-0709, 4 pages, Detroit, MI (2002).
4. Chookazian, S., "Bonding with Electromagnetic Energy", *Assembly*, pp. 38-42 (January 2000).
5. Nichols, R. J., "Advances in the EmabondTM Induction Welding Process for High-Performance Assembly of Demanding Thermoplastics", Assembly Technology Expo Seminar, 10 pages, (September 2003)
6. Stokes, V., "Experiments on the Induction Welding of Thermoplastics", SPE ANTEC Proceedings, **2** 1288-1301 (2001).

Key Words

Induction, electromagnetic, fiber-glass, reinforcement, strength, burst pressure, optimized, load-bearing.

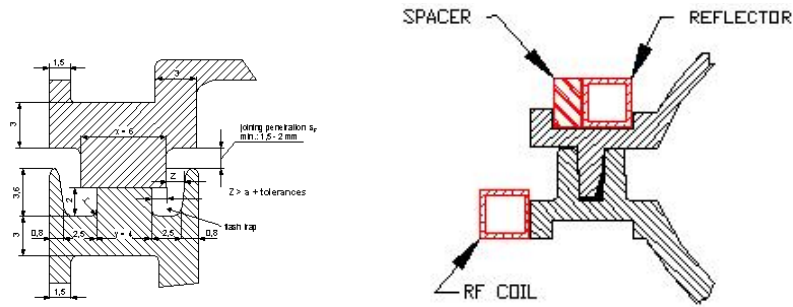


Figure 1. Schematic views of (vibration welding) butt-joint and (induction welding) tongue-in-groove joint

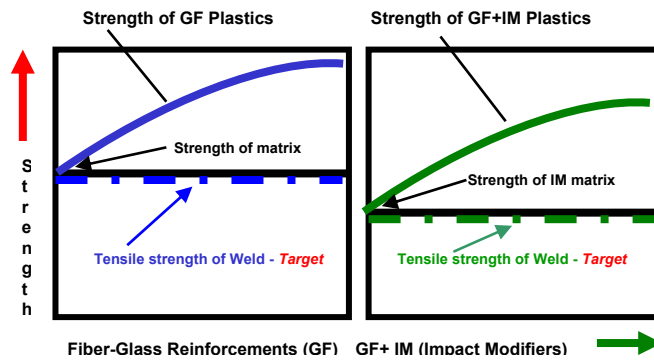


Figure 2. The influence of reinforcements and impact modifiers on tensile strength of welded nylon

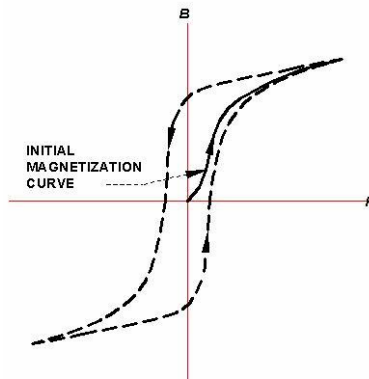


Figure 3. Typical magnetic hysteresis loop

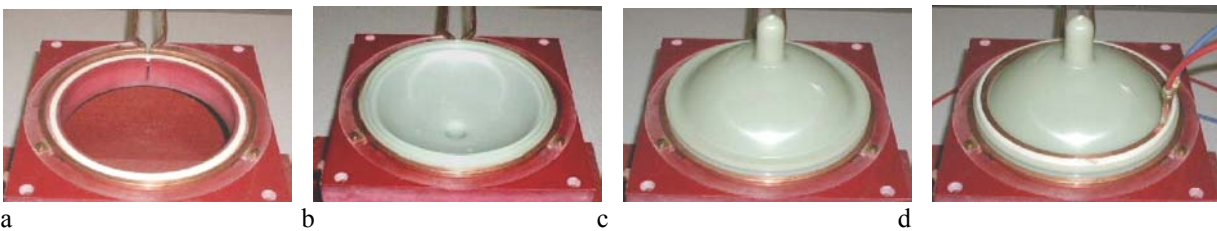


Figure 4. Details of induction welding system: a) RF coil, b) RF coil with lower half of cereal bowl in place, c) RF coil with both halves of cereal bowl in place, d) bowl with upper (reflector) coil positioned relative to the cereal

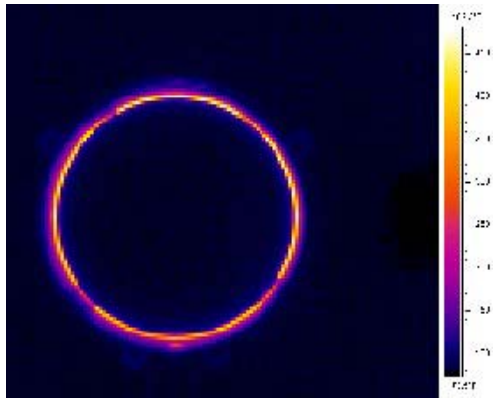


Figure 5. Typical thermal image of lower half of cereal bowl with magnetic implant material in active RF field

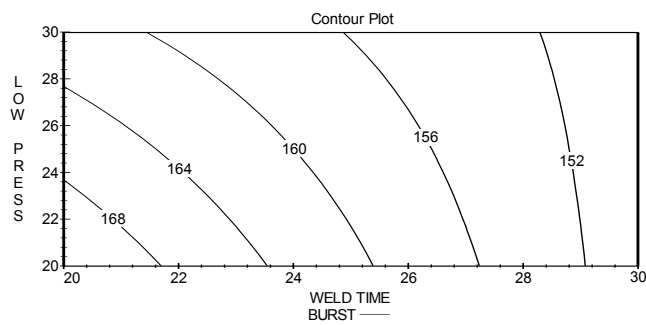


Figure 6. Screening DOE contour plot to establish initial process conditions



Figure 7. Burst strength performance summary



Figure 8. Tongue fractures a) nearer the tip of the tongue, b) nearer the root of the tongue, c) no tongue fracture evident